

## Spatio-temporal Analysis of Sentinel-5P Data of Konya City Between 2019-2021

(2019-2021 Yılları Arası Konya İli Sentinel-5P Verilerinin Mekâna-Zamana Dayalı Analizi)

Hasan Bilgehan MAKİNECİ<sup>1</sup>, Duygu ARIKAN<sup>2</sup>, Damlanur ALKAN<sup>3</sup>, Lütfiye KARASAKA<sup>4</sup>

Konya Teknik Üniversitesi, Mühendislik ve Doğa Bilimleri Fakültesi, Harita Mühendisliği, Konya

\*Sorumlu yazar: hbmakineci@ktun.edu.tr, darikan@ktun.edu.tr, dalkan@ktun.edu.tr, lkarasaka@ktun.edu.tr

Received (Geliş Tarihi): 09.04.2023

Accepted (Kabul Tarihi): 20.07.2023

### ABSTRACT

Uncontrolled energy consumption by human beings, such as the increase in the demand for the gases used for heating purposes in houses, the rise in the number of industrial production facilities, and the uncontrollable levels of the gases emitted from the exhausts of motor vehicles, are among the causes that trigger chemical gas formation in the atmosphere. Increases in air pollution threaten people's health and disrupt ecological balances. For this reason, regularly monitoring the amount of pollution and taking the necessary precautions is crucial. In this study, which was conducted for this reason, the state of polluting gases between 2019-2021 in the province of Konya was examined using remote sensing data. The data were obtained from the TROPOMI instrument attached to the Sentinel-5 Precursor (S5P) satellite launched into orbit by the European Space Agency (ESA). Various atmospheric gases (ozone, methane, carbon monoxide, nitrogen dioxide, sulfur dioxide, and formaldehyde) can be detected by the sensors in this device. For this purpose, S5P Level-2 data was accessed via the Google Earth Engine (GEE) platform, and different codes were written to obtain each data. Then, the data collection for the study region was completed. The monthly amount of carbon monoxide, ozone, methane, and nitrogen dioxide gases for the study area between the specified dates are shown in the graphs, and maps are produced for each year. As a result, it has been determined that methane gas is not observed in extensive wetlands and forest areas, and the minimum values of NO<sub>2</sub>, O<sub>3</sub>, and CO gases are in the summer months and CH<sub>4</sub> gas in the winter months. It has also been determined that the region between the west and the south of the city center is the healthiest region in terms of air pollutant gases.

**Keywords:** Google Earth Engine, Konya Air Quality, Pollutant Gases, Sentinel-5P, TROPOMI Satellite

### ÖZ

Konutlarda ısınma amaçlı kullanılan gazlara olan talebin artması, endüstriyel üretim tesislerinin sayısının artması, motorlu taşıtların egzozlarından çıkan gazların kontrol edilemeyen seviyelere ulaşması gibi insanoğlunun kontrolsüz enerji tüketimi, atmosferde kimyasal gaz oluşumunu tetikleyen nedenler arasındadır. Hava kirliliğindeki artışlar insan sağlığını tehdit etmekte ve çevresel yaşam dengelerini

bozmaktadır. Bu nedenle kirlilik miktarının düzenli olarak izlenmesi ve gerekli önlemlerin alınması gerekmektedir. Bu amaçla gerçekleştirilen bu çalışmada, uzaktan algılama verileri kullanılarak Konya ilinde 2019-2021 yılları arasındaki kirletici gazların durumu incelenmiştir. Veriler, Avrupa Uzay Ajansı (ESA) tarafından yörüngeye fırlatılan Sentinel-5 Precursor (S5P) uydusuna bağlı TROPOMI algılayıcısından elde edilmiştir. Bu algılayıcıdaki sensörler tarafından çeşitli atmosferik gazlara (ozon, metan, karbon monoksit, nitrojen dioksit, kükürt dioksit ve formaldehit) ait zamansal değişim belirlenebilir. Bu amaçla Google Earth Engine (GEE) platformu ile S5P Düzey-2 verilerine ulaşılmış ve her bir veriyi elde etmek için farklı kodlar yazılmıştır. Daha sonra çalışma bölgesi için veri elde etme işlemi tamamlanmıştır. Çalışma alanı için belirlenen tarihler arasındaki aylık karbon monoksit, ozon, amonyak ve nitrojen dioksit gazları miktarları grafiklerde gösterilmiş ve her yıl için haritalar üretilmiştir. Sonuç olarak geniş sulak alanlarda ve ormanlık alanlarda metan gazının görülmediği, NO<sub>2</sub>, O<sub>3</sub> ve CO gazlarının minimum değerlerinin yaz aylarında, CH<sub>4</sub> gazının ise kış aylarında olduğu tespit edilmiştir. İl merkezinin batısı ile güneyi arasında kalan bölgenin havayı kirletici gazlar açısından en sağlıklı bölge olduğu da belirlendi.

**Anahtar Kelimeler:** Google Earth Engine, Kirletici Gazlar, Konya Hava Kalitesi, Sentinel-5P, TROPOMI uydusu

### 1. INTRODUCTION

In recent studies, polluting air emissions have been associated with meteorological conditions and human activities (Balmes, 2019; Cheung, et al., 2020; Kurata, et al., 2020; Lu, et al., 2019; Ghasempour, et al., 2021). The seasonal and temporal analysis of different meteorological parameters, and the relationship between the atmosphere and air temperature in urban areas, has been supported by several studies in the literature (Arıkan & Yıldız, 2022; Ghasempour, et al., 2021; Safarianzengir, et al., 2020; Sager, 2019; Sobhani & Zengir, 2019; Sobhani & Zengir, 2020). Researchers have determined that the primary purpose for this is to determine which factors influence the air temperature in the atmosphere during the day in urban areas. In

addition, as a result of these studies, the factors that cause air pollution events in urban areas are identified.

Air pollution refers to the fact that air pollutants in the atmosphere reach a level above average due to human or natural causes, and their presence in the atmosphere in density, amount, and time that may adversely affect human health, living life, and ecological balance. In other words, it is expressed as the deterioration of the natural composition of the air. Artificial sources of air pollution occur as a result of human activities. As a result of heating, transportation, and industry, there is an increase in the number of pollutants emitted into the atmosphere. Heating boilers and solid, liquid, and gas fuel stoves for heating, ships, motor vehicles, railways, and airplanes in the field of transportation, processes carried out in the industry and power plants that produce thermal and hydraulic energy have a direct negative effect on air pollution (Ibbetson, Symonds, & Hutchinson). In contrast, natural sources of air pollution are natural events (URL-2). Particularly prevalent examples of natural sources are earthquakes, forest fires, volcanic eruptions, dust storms, swamps, oceans, and seas. Air pollutants from natural events do not linger in the atmosphere for long. Investigation of changes in the concentration of carbon monoxide, nitrogen dioxide, ozone, and methane, known as air pollutants, is seen as a threat to human health, the ecosystem, biodiversity, and climate (Safarianzengir et al., 2020). For this reason, monitoring polluting gases and examining their effects on humans and the environment is necessary.

High-resolution Sentinel-5P (S5P) TROPOMI satellite data have recently gained popularity in air quality monitoring research (Singh et al., 2021; Wang, et al., 2022). The S5P, developed to use institutes in the Netherlands, the United Kingdom, Finland, and Germany for scientific studies, was launched into orbit in 2017 on a seven-year operation (Farahat, 2022). The satellite data have a spatial resolution of  $3.5 \times 5.5$  km and a temporal resolution with daily periods (Theys et al., 2017). Thanks to this remote sensing platform, spatial and temporal analyzes, and monitoring of air quality variability are carried out more comprehensively. Griffin et al. (2019) found a high correlation between the vertical column density of  $\text{NO}_2$  gas and ground-based observations. In the study by Wang et al. (2022),  $\text{NO}_2$ ,  $\text{CO}$ , and  $\text{CO}_2$  gases were used to compare the data results produced by ground observations and remote sensing techniques (Ghasempour et al., 2021a;

Ghasempour et al., 2021b). Makineci (2022) conducted a study on the region's air pollution by using S5P data and terrestrial stations on the Anatolian and European parts of İstanbul, the metropolitan city of Türkiye. As a result of the study, in which ground stations and remote sensing data were used, consistent results were revealed for two different centers of air pollution. Stratoulis and Nuthammachot (2020) found a strong positive correlation between data from ground stations for an urban area and data from S5P.

In line with the findings obtained from the studies, the consistency of the terrestrial and remote sensing data in determining anthropogenic emissions is observed. As a result, it has been concluded that satellite images can be used to detect pollutants, present the spatial distribution of gases and particles that cause air pollution, cover large areas, and provide repeated measurements due to the cost of establishing ground-based stations in the studies. In addition, S5P satellite data have benefited from the amount of gas released into the atmosphere and find solutions to the problems such as in studies on forest fires (Arikan & Yıldız, 2023; Singh et al., 2021), in the detection of oil refineries and fields (Farahat, 2022), and in explaining the relationship between air pollution and diseases (Arikan & Yıldız, 2021; Balmes, 2019; Ibbetson et al., 2020; Kurata et al., 2020; Lu et al., 2019).

Since air pollution is a global issue, the whole world must reduce their emissions of polluting gases to the minimum level locally. For this purpose, a comprehensive analysis of air pollution in Konya, Türkiye's largest city, was carried out to contribute to the literature. Temporal and spatial analyzes of methane ( $\text{CH}_4$ ), ozone ( $\text{O}_3$ ), carbon monoxide ( $\text{CO}$ ), and nitrogen dioxide ( $\text{NO}_2$ ) gases, which are the primary air pollutants within the borders of Konya Province, were conducted between July 2019 and December 2021, using the Google Earth Engine (GEE) platform and the obtained S5P data. The air quality of Konya province was monitored monthly between 2019-2021 by dividing the data into separate equal grids ( $25 \times 25$  m). It has been attempted to determine the increase or decrease of the pollutants in the 30-month period and the responsible factor. The fact that there is no other research in the literature that maps the air pollutants of Konya for such a long period by using the GEE platform on the S5P satellite since the data began to be published to the users encouraged this study. The density of the data, the long-term spatio-temporal analysis,

and the study's wide scope can be said to be the study's original aspect.

## 2. MATERIALS AND METHODS

### a. Study Area and Workflow

Konya which is located in the Central Anatolia region of Türkiye and has the largest surface area (38 873 km<sup>2</sup>), was chosen as the study area. The city is located between 36°41' and 39°16' north latitudes and 31°14' and 34°26' east longitudes (Figure 1).

In the city, which is influenced by the continental climate, the summer is dry and hot, while the winter is extremely cold and has heavy snowfall. Rainfall is seen throughout the city in the spring and winter seasons. The city is located at an altitude of 1016 m above sea level. Due to the mountains surrounding the city, the effect of the wind is limited and causes fog/smoke condensation in the city (Kunt & Dursun, 2016). This causes polluted air to accumulate in the city.

According to 2022 population data, it is Türkiye's sixth most populous city, with 2 296 347 people. Although the primary economic income source of the region is known as agricultural production, it has also acquired the reputation of an industrial production city due to the increasing industrialization in recent years. The city trades quickly with other central provinces in the country thanks to its widespread transportation lines. It also contributes to the national economy by producing goods in a variety of sectors (agricultural machinery and equipment, defense and automotive industry, food, etc.).

While these factors contribute to the development of the city, their effects on air-polluting gases should also be identified. For this reason, in this study, the air pollution of Konya province was investigated temporally and spatially by using S5P satellite data. Sentinel-5 data of NO<sub>2</sub>, CO, O<sub>3</sub>, and CH<sub>4</sub> polluting gases were obtained from the GEE platform within the specified date range for analysis.

Each gas with the same temporal and spatial resolution used in the study has been analyzed with charts, then visualized and represented on maps. The workflow diagram of the study is presented in Figure 2.

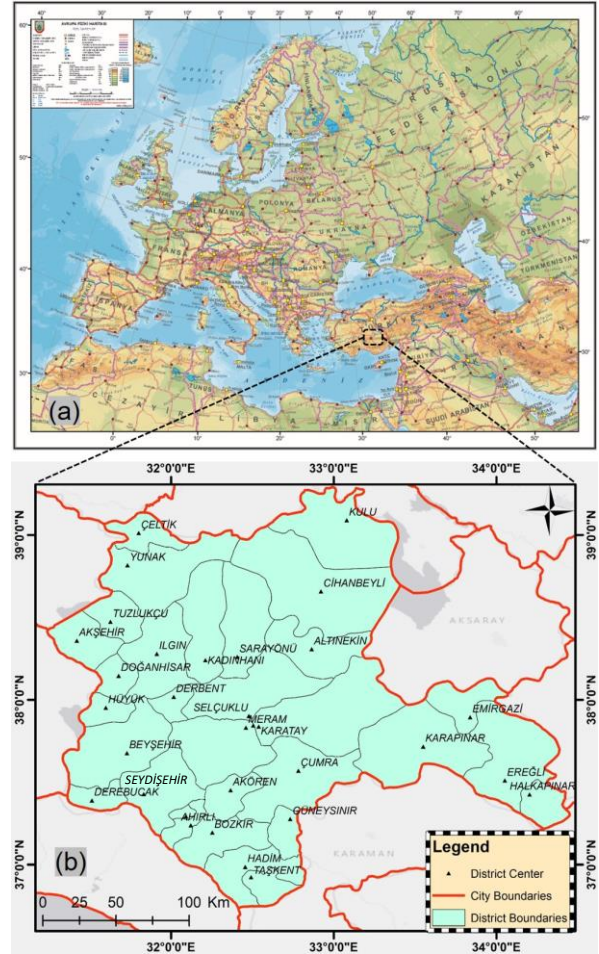


Figure 1. (a) (b) Study area (Figure 1. (a) Produced by the General Directorate of Mapping))

### b. S5P Data

The data obtained from the TROPOMI device connected to the Sentinel-5 satellite by the European Space Agency was used in this study. Various atmospheric gases (ozone, methane, carbon monoxide, nitrogen dioxide, sulfur dioxide, and formaldehyde) are detected and monitored by the sensors in this device (Slagter, et al., 2020; Veeffkind et al., 2012). The satellite's primary purpose, launched on October 13, 2017, is to collect atmospheric measurements with high spatio-temporal resolution for air quality, ozone, UV radiation, climate monitoring, and forecasting (Safarianzengir et al., 2020). It scans the Earth daily and records images with a coverage area of 7 km × 3.5 km. The satellite, expected to have a seven-year operational life, is in the low-orbiting satellite class with an orbital reference altitude of 824 km. It is in a sun-synchronous orbit with the equatorial transit at the nodal point rising at 13:30 local time, with an orbital inclination of approximately 98.7 degrees in polar orbit. The

orbital cycle is 16 days. The satellite is equipped with the most advanced TROPOMI instrument for measuring the ultraviolet-visible (270–500 nm), near-infrared (675–775 nm), and short-wave infrared (2305–2385 nm) spectral bands (Rohi & Ofualagba, 2020; Safarianzengir et al., 2020). The TROPOMI spectrometer in Sentinel 5P measures high spectral UV luminance (<https://sentinels.copernicus.eu/web/sentinel/missions/sentinel-5p>). The download of Sentinel-5P Level-2 data was carried out through the GEE platform, an infrastructure of Google. A separate coding process was carried out for each pollutant gas. L2 level data received from the Sentinel satellite is defined at the L3 level through GEE. Therefore, Spatial Resolution corresponds to around 1 km. This platform is a web service developed for spatial analysis (Gorelick et al., 2017). It has gained popularity in remote sensing studies in recent years because it is free to use and provides easy access to data (Farahat, 2022; Singh et al., 2021). In addition, GEE (Li et al., 2022), which enables extensive data processing, offers its users the opportunity to create and save their catalogs. Query and evaluation processes are also carried out through the functional structures in the system (Gorelick et al., 2017).

The NO<sub>2</sub> (nitrogen dioxide) vertical column, CH<sub>4</sub> (methane) column average dry air mixing ratio, total O<sub>3</sub> (ozone) atmospheric column between the surface and upper atmosphere, and CO (carbon monoxide) column data for 2019-2021 are downloaded as offline (OFFL). This is primarily because it should contain data from a single orbit. Additionally, only the OFFL feature is available for CH<sub>4</sub> data. In this study, data on certain monthly days were downloaded for each gas using the median code in GEE. This path was followed as there was a lack of data on certain days for some

gases. From 2019 to 2021, 118 images were obtained for all of the used gases. Then, the downloaded images were opened in the GIS environment and visualized (Figure 11, Figure 12, Figure 13, Figure 14 and Figure 15).

In order to eliminate the gaps seen in the methane gas daily data and to create a standard for all gases, a three-day data format was downloaded. Three-day data yield more meaningful results, so the gaps in the daily data are not filled with interpolation, based on the principle of producing maps entirely from S5P sensor data. In the GEE platform, there is a pre-acceptance assumption that the data will be downloaded for three days.

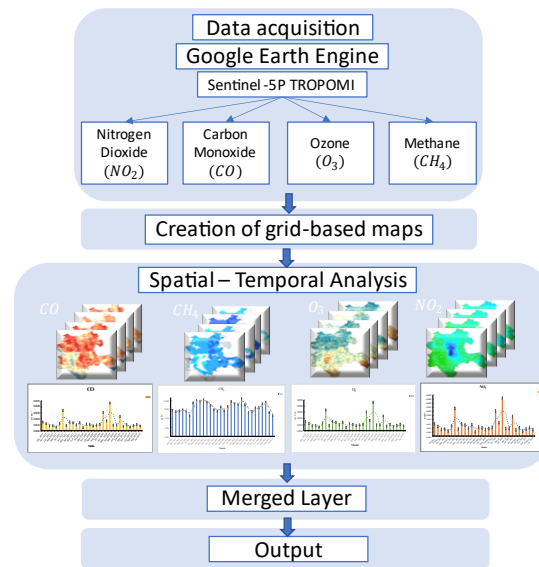


Figure 2. Workflow of research

**Table 1.** Sentinel-5P data used in research.

Data Type	Temporal Resolution	Spatial Resolution	Calibration Type
O <sub>3</sub>	First 3 days of every month	1113.2 meters	Radiometric and Geometric Calibrated
CH <sub>4</sub>	First 4 days of every month	1113.2 meters	Radiometric and Geometric Calibrated
CO	First 10 days of every month	1113.2 meters	Radiometric and Geometric Calibrated
NO <sub>2</sub>	First 10 days of every month	1113.2 meters	Radiometric and Geometric Calibrated

### c. Statistical analysis

After obtaining the data, all visual base maps were gridded after trimming, and classification processes were applied to the leading data visualized in the GIS environment. The value corresponding to the midpoint of each grid was then calculated. Following the calculation, the thirty-month data of the values corresponding to the grid midpoints according to the months were tabulated. In Table 1, there are blank values for different data types in some months of the data consisting of 332 points. Gaps without data were not included in the statistical analysis of the study. No interpolation was applied to the non-data regions, and their values were left as naught.

Among the values obtained in Table 1, the maximum, minimum, mean, and median values were determined according to each data type. Additionally, standard deviation (StD.) values were calculated for the analysis.

## 3. RESULTS

### a. Findings Obtained for CH<sub>4</sub> Gas

Methane gas (CH<sub>4</sub>) is the greenhouse gas with the most critical polluting effect after carbon dioxide (Hu et al., 2018). Therefore, it is a type of gas that causes global warming at a higher rate than other pollutants (Stocker, 2014). CH<sub>4</sub> gas is emitted into the atmosphere, either by natural or anthropogenic resources. Anthropogenically, it

can be expressed as oil and natural gas systems, agricultural activities, coal mining, stationary and mobile incineration, wastewater treatment, and specific industrial processes. Swamps can be an example of natural causes (Lorente et al., 2021). Thanks to the near-infrared (NIR) and short-wave infrared (SWIR) spectral bands found in satellites, CH<sub>4</sub> gas is observed through its spread on the Earth's surface and atmosphere. Data from TROPOMI measurements are recorded with the RemoTeC algorithm (Lorente et al., 2021). The residence time of this gas in the atmosphere has been determined as approximately ten years (Hu et al., 2018).

When the July 2019 - December 2021 data for the whole of Konya were examined (Figure 3), it was determined that the highest amount of CH<sub>4</sub> was in September 2021, with 1900 mg/m<sup>3</sup>. When the maximum and minimum values of methane gas are examined within each month, it is understood that the mean is 40 mg/m<sup>3</sup>. Since methane gas is seen primarily as a result of heating, there is a standard distribution across urban areas. In addition, it has been determined that CH<sub>4</sub> release is not significantly affected by season because a balanced graphic curve was obtained in the summer and winter seasons.

In the time period of the study, 6,925 mg/m<sup>3</sup> minimum StD. values in July 2021 and 12,658 mg/m<sup>3</sup> maximum StD. values in April 2020 were determined (Figure 4).

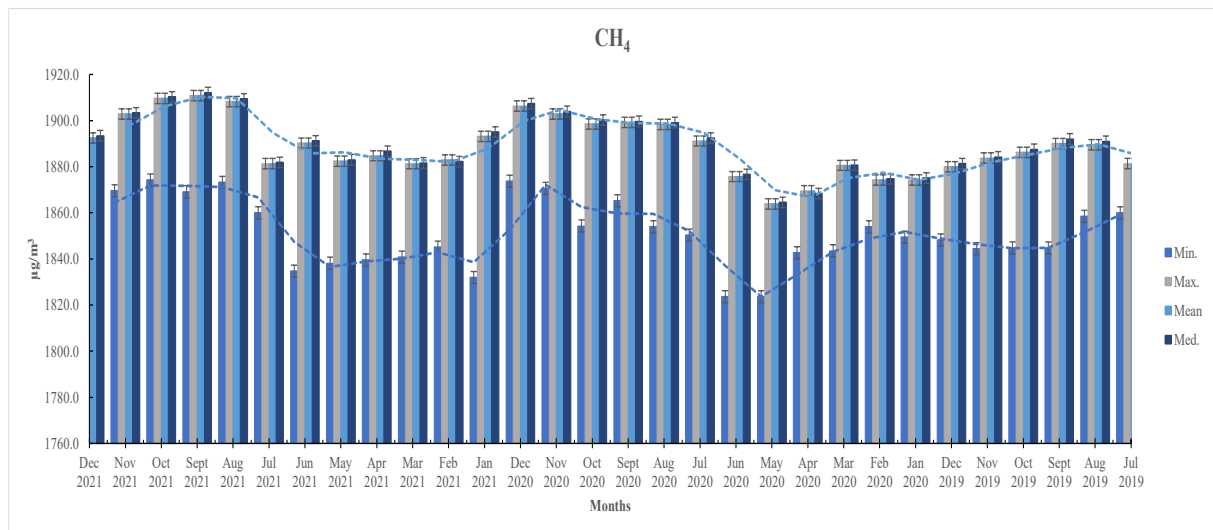


Figure 3. CH<sub>4</sub> Data Analysis (Minimum, Maximum, Mean and Median Values)

**b. Findings Obtained for CO Gas**

CO gas remains in the atmosphere for less time (by approximately two months) than methane gas. It is a product of incomplete combustion encountered in building heating, coal power generation, wood and grass burning, vehicles, and biomass burning (Ghahremanloo, Lops, Choi, & Mousavinezhad, 2021). About 40% of CO is naturally generated (volcanic eruptions, natural gas emissions, degradation of plants and animals, forest fires, and 60% results from the consumption of fossil fuels, garbage disposal systems, tobacco smoke, and coal fires (Kaplan, Avdan, & Avdan, 2019). Graphs were created each month from the CO findings obtained to cover the entire study area. Monthly maximum, minimum, mean and median values are given in Figure 5, and StD.

values are presented in Figure 6. The highest amount of CO in the monthly period was determined in April 2020, and the maximum was reached with a value of 0.1818 mol/m<sup>2</sup> in that month. The lowest amount of CO in the study period was recorded in November 2020, with a value of 0.1255 mol/m<sup>2</sup>. It is worth mentioning that the change in temperature because, as can be seen from the graph, while there is a decrease in the amount of CO in the winter, it increases in the summer.

According to the StD. values of CO gas, it reached maximum levels of 0.0042 mol/m<sup>2</sup> in the same period (April 2020) as methane gas. It has been detected at a minimum in December 2020 with 0.0005 mol/m<sup>2</sup>.

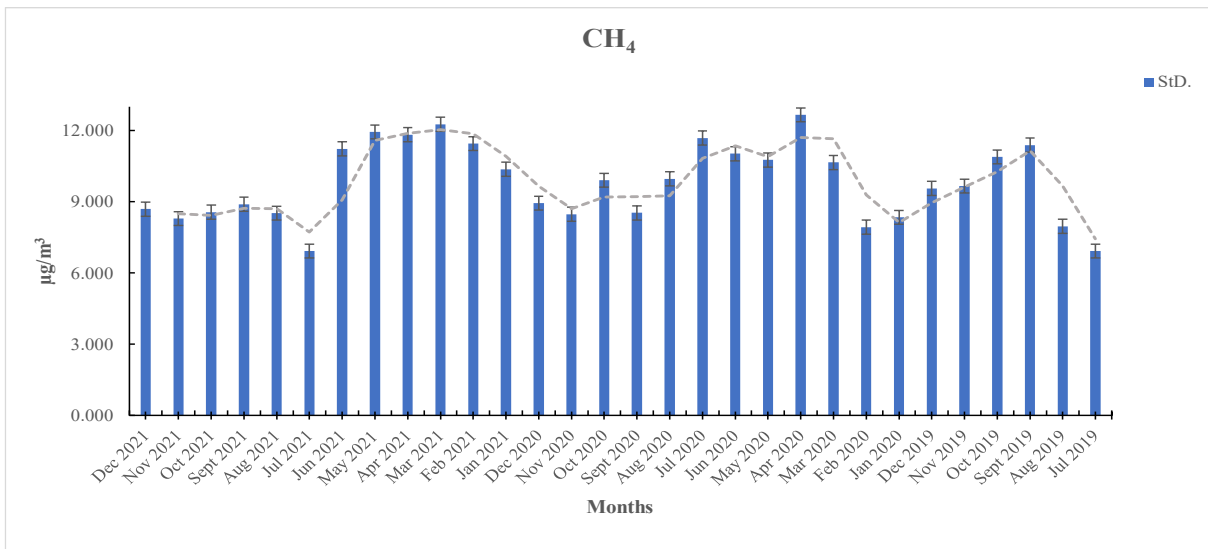


Figure 4. CH<sub>4</sub> Data Analysis (StD. Values)

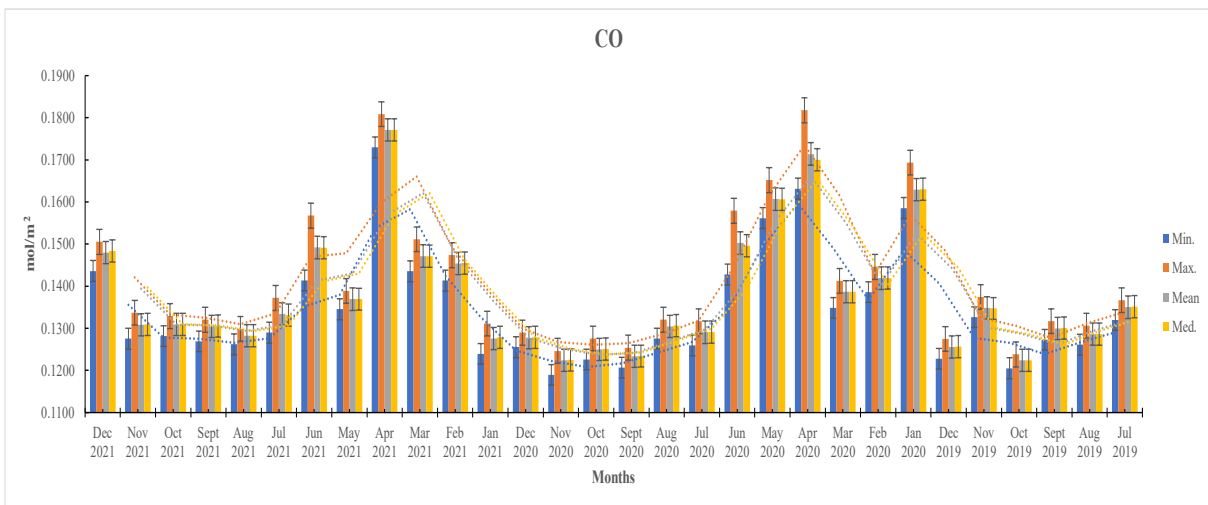


Figure 5. CO Data Analysis (Minimum, Maximum, Mean and Median Values)

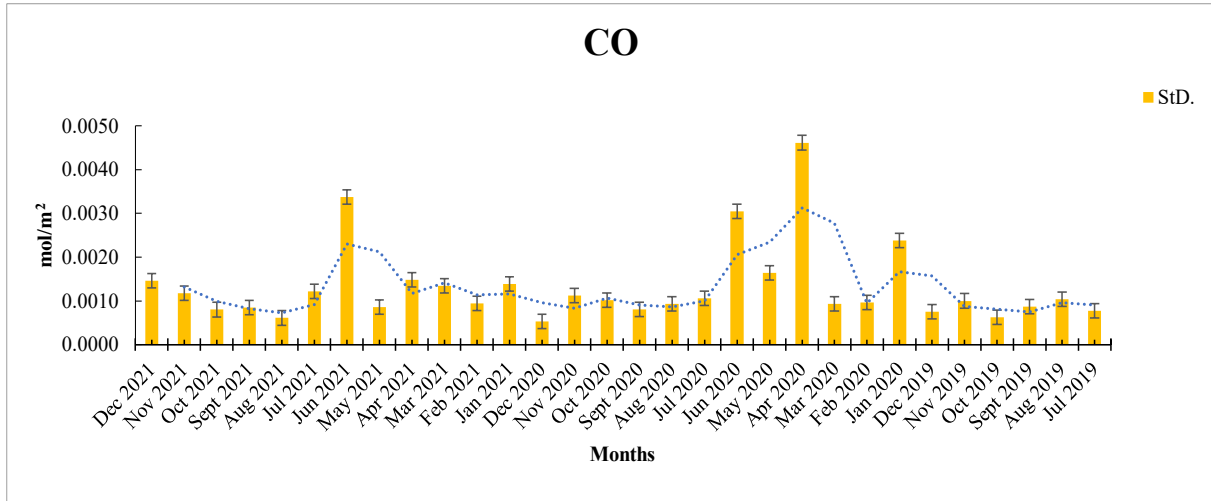


Figure 6. CO Data Analysis (StD. Values)

### c. Findings Obtained for NO<sub>2</sub> Gas

Nitrogen oxides (NO<sub>x</sub>) are generally the type of gas that occurs during combustion (Ialongo, Virta, Eskes, Hovila, & Douros, 2020). The leading sources of this type of gas are natural (lightning strikes) and anthropogenic pollution (burning of agricultural fields, burning fossil fuels, industrial production, and emissions from vehicle exhaust) sources (Hashim, et al., 2021; Ialongo et al., 2020).

NO<sub>2</sub> gas increases the symptoms of respiratory diseases (such as coughing, wheezing, or difficulty breathing) by affecting human health (Stratoulis & Nuthammachot, 2020). In addition, it causes acid rain by interacting with water, oxygen, and other chemicals in the atmosphere (Hashim et al., 2021). This occurrence weakens the soil and reduces productivity in agricultural activities. In areas where nitrogen dioxide increases, the air becomes hazy, and there is even a decrease in visibility.

Figures 7 and 8 display the time series of NO<sub>2</sub> measurements used in the analysis, covering the period from July 2019 to December 2021. In Figure 7, the maximum, minimum, median, and mean values of the daily monthly data are given, while in Figure 8, the StD. the graph is shown. While the maximum level of NO<sub>2</sub> in the studied period was observed in April 2020 with a value of 0.18176 mol/m<sup>2</sup>, the minimum level was observed in November 2020 with a value of 0.11895 mol/m<sup>2</sup>. It can be said that there is a seasonal effect in NO<sub>2</sub> gas. As shown in Figure 7, while there is an increase in the amount of this gas in the spring season (April, May), there is a decrease in the autumn season (October, November). According

to the StD. values in 30 months, A minimum of 0.0005 mol/m<sup>2</sup> was obtained in December 2020, and a maximum of 0.0046 mol/m<sup>2</sup> was obtained in April 2020.

### ç. Findings Obtained for O<sub>3</sub> Gas

The O<sub>3</sub> concentration commonly found in the air consists of the photochemical interaction of the precursor gases (nitrogen oxides, volatile organic compounds) (Hashim et al., 2021). In cases of exposure to O<sub>3</sub> gas, airway inflammation, and respiratory disorders can be observed in living things due to oxidative stress (Adhikari & Yin, 2020). The magnitude and rate of O<sub>3</sub> emissions depend on atmospheric conditions and seasonal factors (Hashim et al., 2021).

O<sub>3</sub> emission appears to be directly proportional to NO<sub>x</sub>. If O<sub>3</sub> is high in a region, NO<sub>x</sub> is also found to be high, or vice versa (Hashim et al., 2021). On the other hand, while the amount of NO<sub>x</sub> is high in urban areas with high traffic density, reductions in O<sub>3</sub> emissions are observed. This is because the gas density in urban areas is transported toward rural areas (Dentener et al., 2020). Due to the increase in temperatures and the contribution of sun rays to the formation of O<sub>3</sub>, seasonal changes cause a decrease in O<sub>3</sub> gas (Stratoulis & Nuthammachot, 2020). As determined in Figure 9, while O<sub>3</sub> was at its maximum levels in April 2020 and 2021, it appears to have been at minimum levels in October, November, and December. When the StD. values for O<sub>3</sub> are examined (Figure 10), the minimum value of 0.0004 mol/m<sup>2</sup> and maximum value of 0.0040 mol/m<sup>2</sup> were obtained in December 2020 and April 2020, respectively.

When the results of the Std. values of all gases are examined, it can be determined that the

maximum and minimum values of all gases are observed in the same months. In all gases, the maximum level was reached in April 2020. While

the minimum CO, NO<sub>2</sub>, and O<sub>3</sub> gas are December 2020, the time when CH<sub>4</sub> gas is minimum is July 2021.

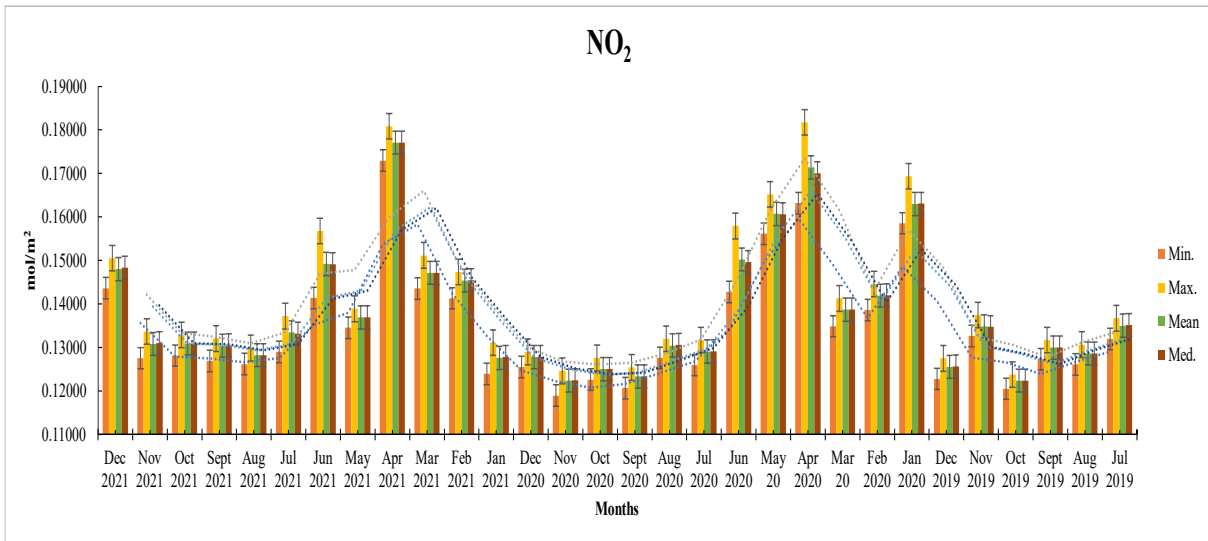


Figure 7. NO<sub>2</sub> Data Analysis (Minimum, Maximum, Mean and Median Values)

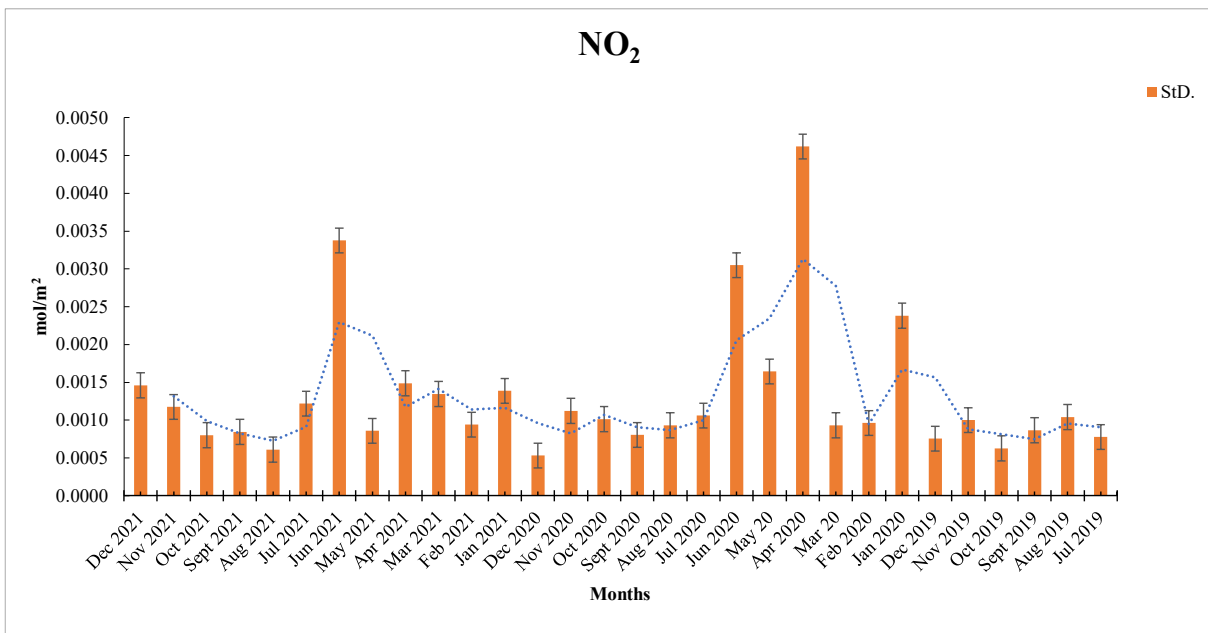
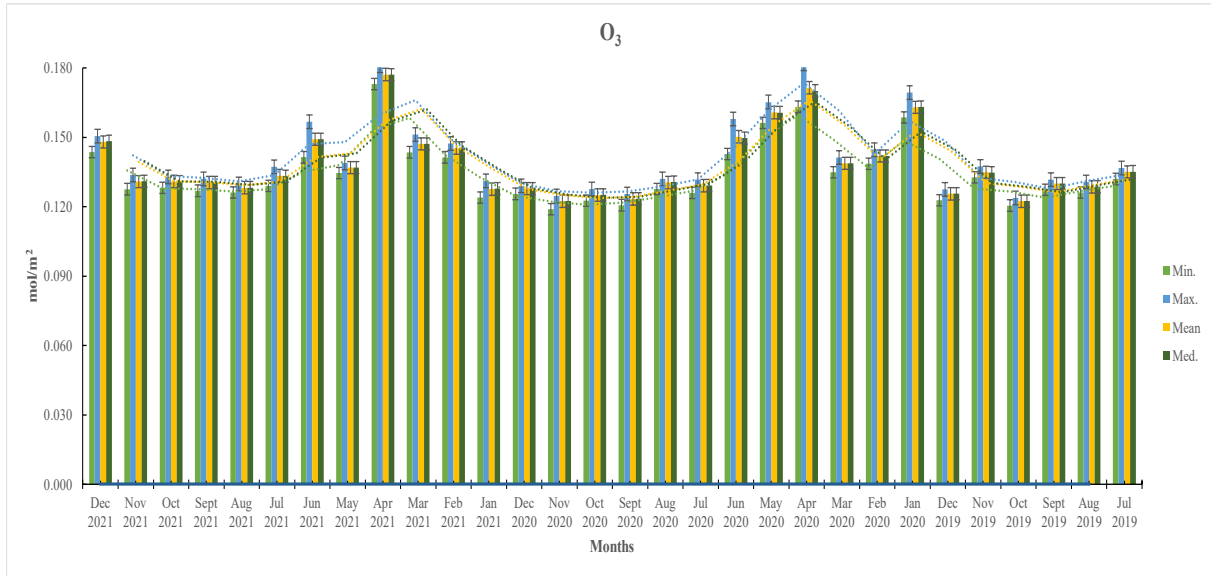
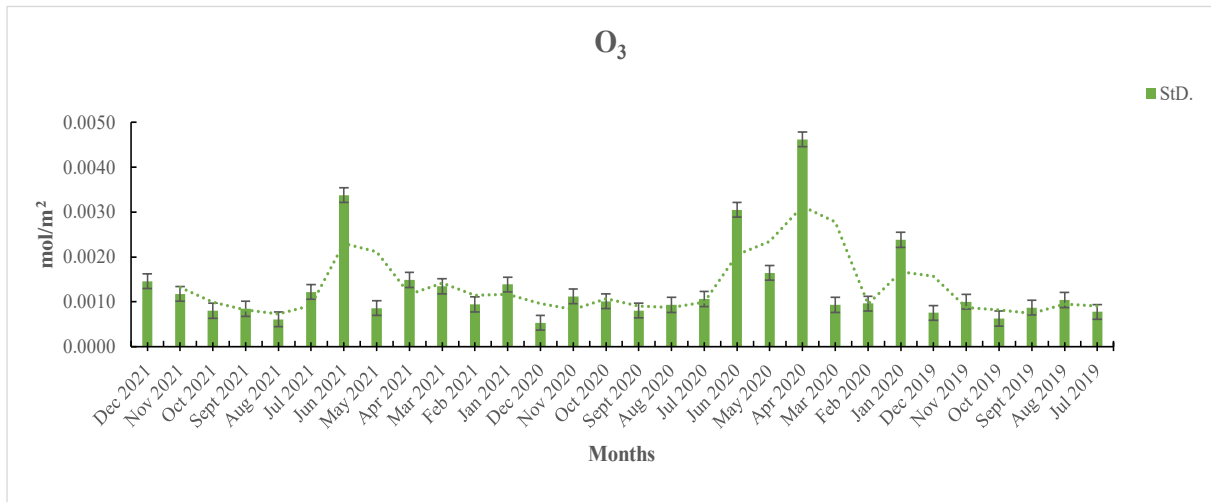


Figure 8. NO<sub>2</sub> Data Analysis (StD. Values)



Figure 9. O<sub>3</sub> Data Analysis (Minimum, Maximum, Mean and Median Values)Figure 10. O<sub>3</sub> Data Analysis Results (StD. Values)

#### d. Produced Map Outcomes

In this study, S5P satellite images taken from the GEE platform were converted to raster and vector maps in order to interpret the air pollutants in the Konya Province in spatio-temporal time. In order to determine the seasonal effect of all polluting gases used in the study, map outputs were produced by choosing the beginning of spring and the beginning of autumn. The most striking point is that the amount of polluting gas is high in the parts of the transportation networks on all maps. It can be said that pollutants vary according to the seasons and are also related to latitude, longitude, and altitude values.

When the CH<sub>4</sub> gas map is examined between the years 2019-2021, it is seen that no data is recorded in the wetlands. The main reason for this is that the effect of methane gas is mainly seen in swamps, reeds, or garbage areas. When the maps of NO<sub>2</sub> and O<sub>3</sub> gases are examined, it has been determined that the amount of NO<sub>2</sub> is high and the amount of O<sub>3</sub> is low in the parts where the transportation lines are located. It has been determined that O<sub>3</sub> emissions are primarily concentrated in rural areas. As seen in Figure 11, while the amount of O<sub>3</sub> gas increases relatively in rural areas in the northern parts of the city, it is found in lower amounts in the southern parts of the city where the altitude is high.

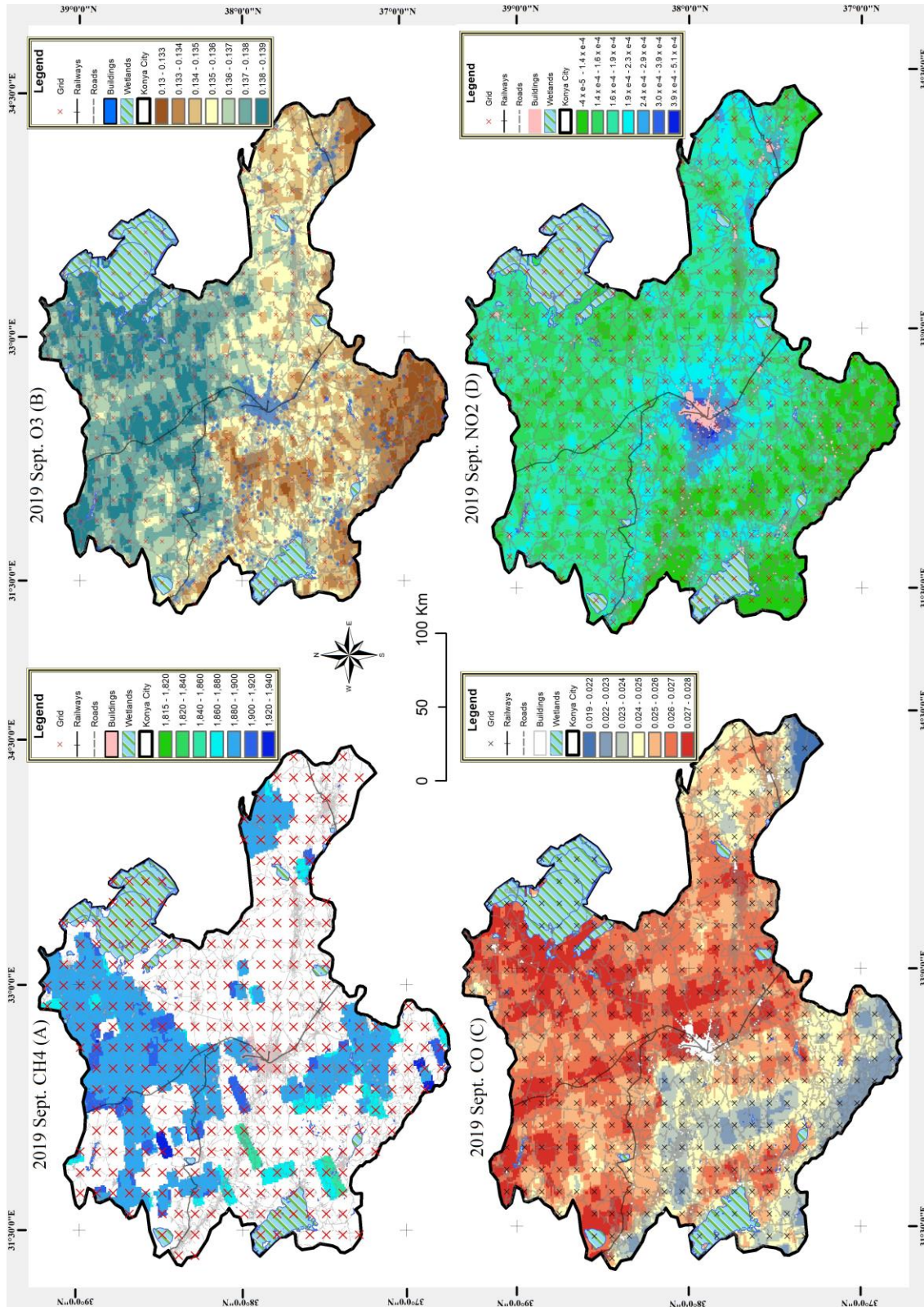


Figure 11. September 2019 Air Quality Map of Konya (A-CH<sub>4</sub>, B-O<sub>3</sub>, C-CO, D-NO<sub>2</sub>)

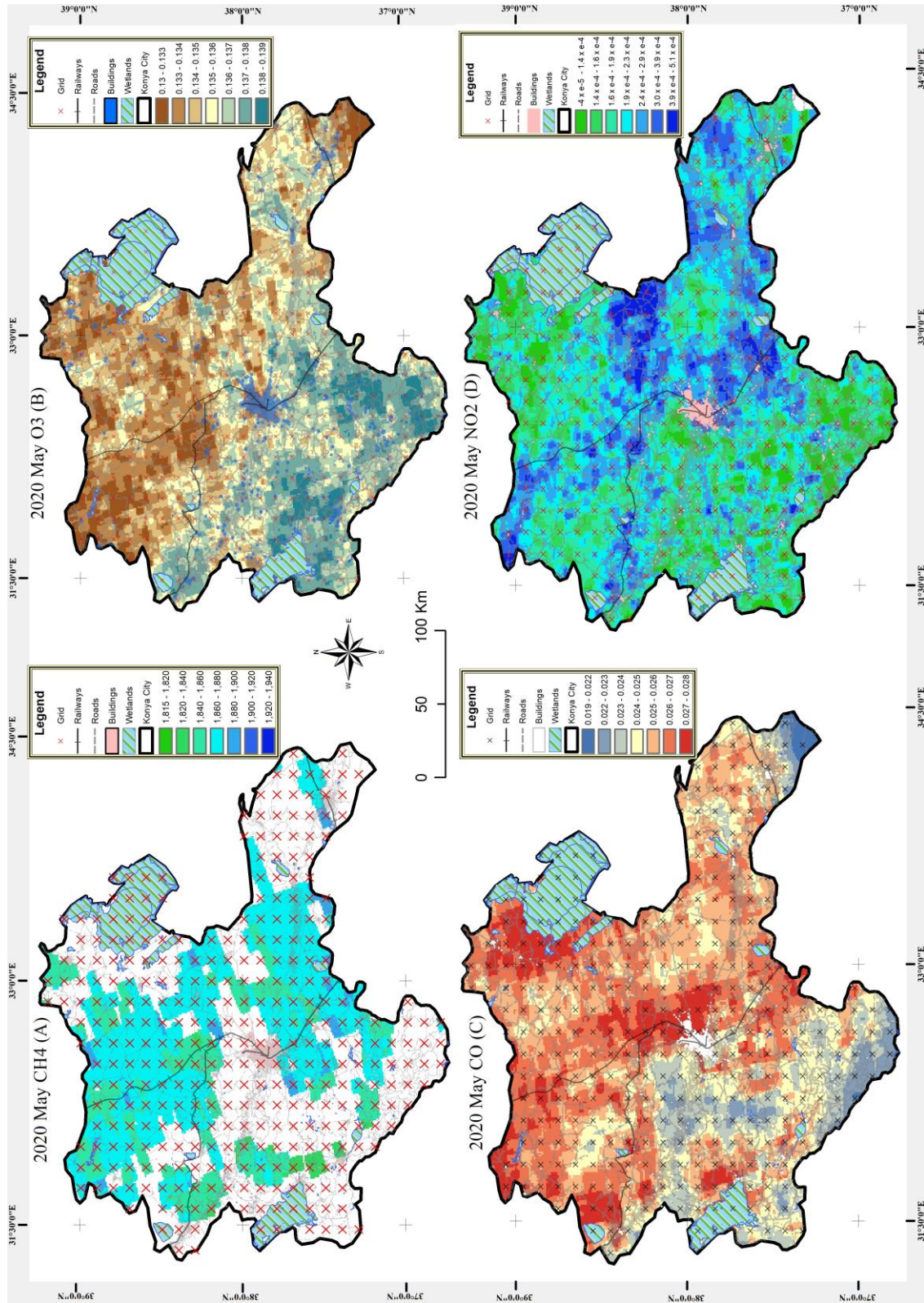


Figure 12. May 2020 Air Quality Map of Konya (A-CH<sub>4</sub>, B-O<sub>3</sub>, C-CO, D-NO<sub>2</sub>)

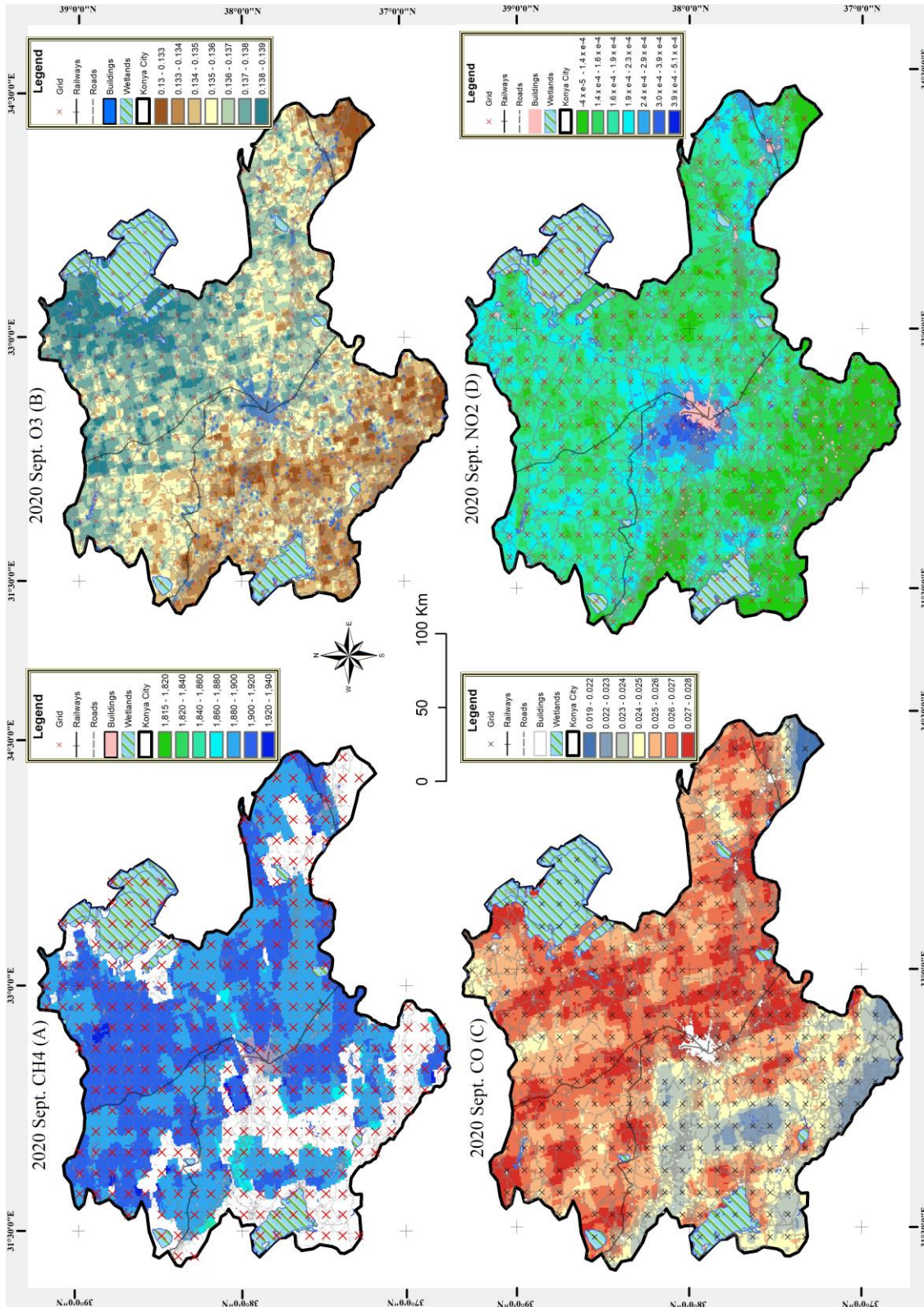


Figure 13. September 2020 Air Quality Map of Konya (A-CH<sub>4</sub>, B-O<sub>3</sub>, C-CO, D-NO<sub>2</sub>)

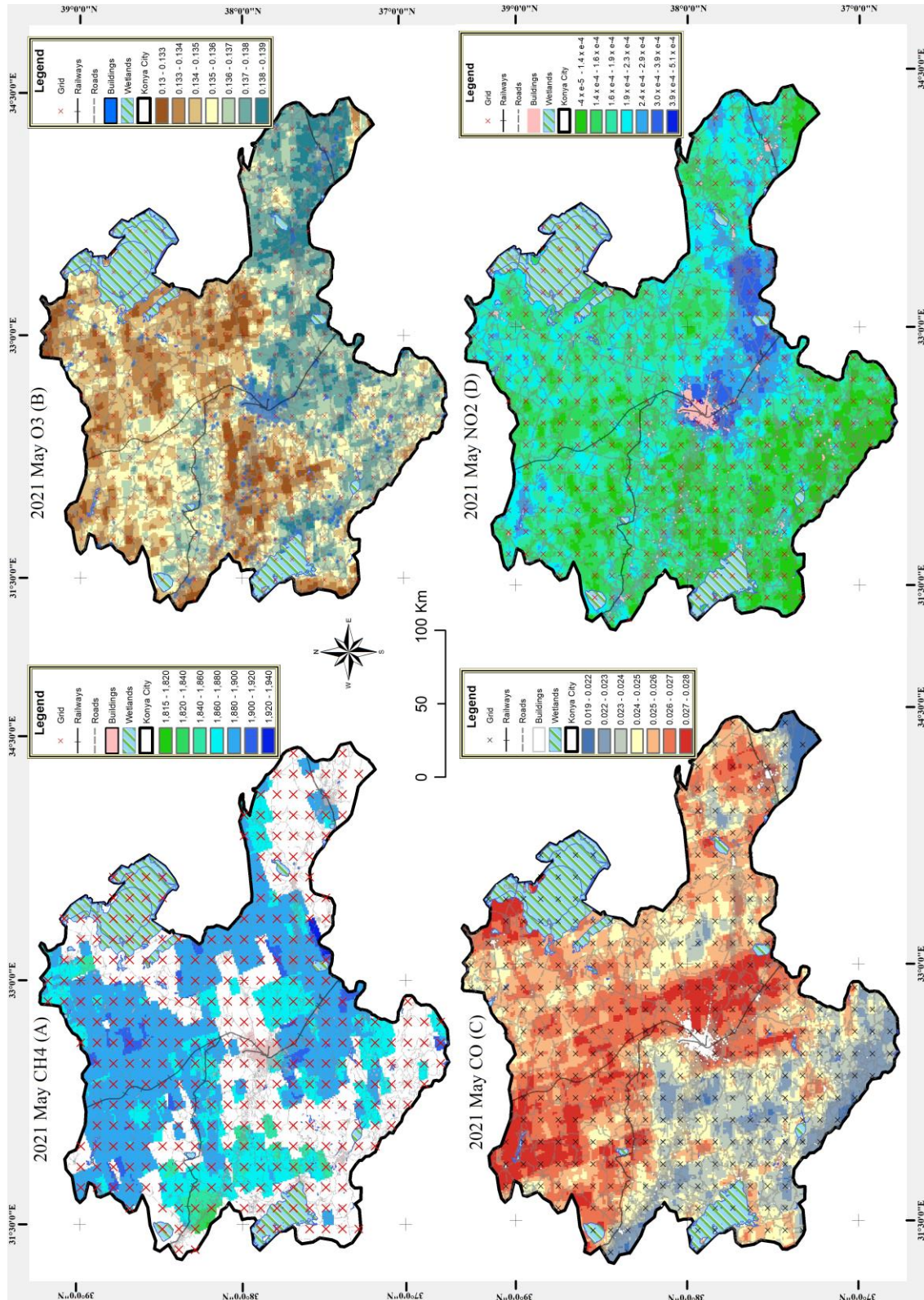


Figure 14. May 2021 Air Quality Map of Konya (A-CH<sub>4</sub>, B-O<sub>3</sub>, C-CO, D-NO<sub>2</sub>)

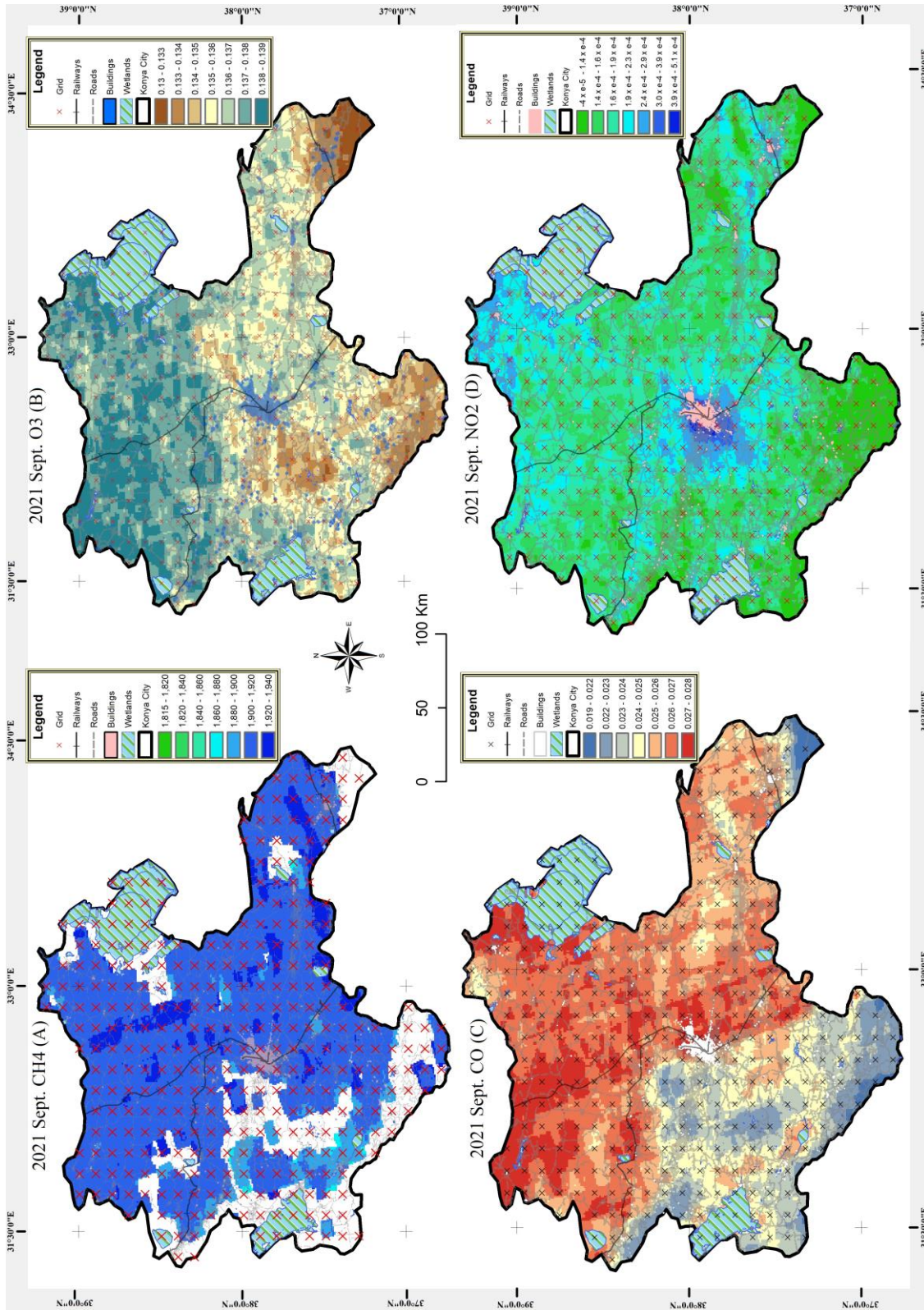


Figure 15. September 2021 Air Quality Map of Konya (A-CH<sub>4</sub>, B-O<sub>3</sub>, C-CO, D-NO<sub>2</sub>)

The amount of all pollutants in 2020 is less than in other years. This is due to the epidemic disease (COVID-19), which spread worldwide during this period, showing its impact on Türkiye. As a result of the restrictions put in place to prevent the spread of the epidemic, it was determined that the impact of the pollutant gases decreased. It has also been determined that the number of pollutants in 2021 were higher than in other years (Figure 12 and Figure 13). This rise has also become meaningful due to the gradual removal of the measures taken for the epidemic. In 2020, methane gas was standard in the northern part of the city. The white parts in the methane gas map are the part where the data is not recorded. Kadınhanı, Sarayönü, and Yunak are the districts where methane gas is seen at high levels. When the methane gas values in March 2021 are examined, it is seen that there are increases in the Karapınar district. Since this region is a reed and swamp area, methane gas increased due to the decrease in water and the resulting drought (Figure 14 and Figure 15).

The situation of four polluting gases over a 30-month period has been examined using satellite data. In the study, national air quality ground station data were also downloaded. However, due to the lack of data on ground stations, it was not used in the analysis. In this study, analyses and discussions were carried out using only S5P satellite data due to factors such as missing terrestrial station data (disorder in stations) or stations representing a spatially narrow region.

#### 4. DISCUSSIONS

The air quality in the atmosphere decreases because the smoke content that results from the combustion of fuels such as diesel and gas pollute the environment from factories and houses in winter, including the pollutants that are the subject of the research. In addition, pollutants are observed more intensely in the atmosphere in winter due to the effect of wind (air reversal phenomenon) compared to warmer seasons. When the gases released in the winter and those released in the summer are compared, it has been determined that the pollutants in hot weather are much more dangerous in terms of air quality. This is because gases such as NO<sub>2</sub> from motor vehicles accumulate in the lower parts of the atmosphere during the summer months, and this is a factor that directly affects human health.

In the study (Ghasempour et al., 2021b) conducted to detect and analyze NO<sub>2</sub> gas from S5P data, researchers were able to notice a

significant correlation between the COVID-19 outbreak and NO<sub>2</sub> gas. In addition, in their analysis on a national basis, they found that NO<sub>2</sub> gas showed a considerable decrease in the lockdown period, except for regular periods (Ghasempour et al., 2021a).

In their study, Kaplan et al. (2019) and Ghasempour et al. (2021) examined country-based polluting gases. Thus, using the Sentinel-5P satellite, they showed that the pollution of a large-scale region could be detected. This study discussed the temporal analysis of the states of polluting gases in small-scale cities, and their detectability was revealed. In addition, more gases were analyzed together, and their relations with each other were established. As in this study, the GEE platform was used to obtain the data. It has been seen that GEE is easy to use and access data, and it can be preferred for accessing S5P data in future studies.


#### 5. CONCLUSIONS

In recent years, air quality research has become one of the critical research topics due to the increase in air pollution, the adverse effects of air pollution on living health, and the availability of rapid and reliable evaluation of air quality with remote sensing satellites. The findings are of great importance to everyone because of the issue's impact on human health and ecological order. Clean air is a vital element for the survival of all living things. For this reason, in this study, the pollutant gases in the Konya province were analyzed temporally and spatially using S5P satellite data from July 2019 to March 2021. As a result, over a 30-month period, the regions in which the pollutants are found and the months when the pollutants are at maximum and minimum levels have been determined. It has been documented that it is possible to collect information about pollutants not only temporally but also spatially, thanks to satellite data.

#### ORCID

Hasan Bilgehan MAKİNECİ 

<https://orcid.org/0000-0003-3627-5826>

Duygu ARIKAN  <https://orcid.org/0000-0001-9976-7479>

Damlanur ALKAN  <https://orcid.org/0000-0002-2013-0262>

Lütfiye KARASAKA  <https://orcid.org/0000-0002-2804-3219>

## REFERENCES

- Adhikari, A., & Yin, J. (2020). Short-term effects of ambient ozone, PM<sub>2.5</sub>, and meteorological factors on COVID-19 confirmed cases and deaths in Queens, New York. *International Journal of Environmental Research and Public Health*, 17(11), 4047. doi:<https://doi.org/10.3390/ijerph17114047>
- Arikan, D., & Yıldız, F. (2023). Investigation of Antalya forest fire's impact on air quality by satellite images using Google earth engine. *Remote Sensing Applications: Society and Environment*, 109922. doi:<https://doi.org/10.1016/j.rsase.2023.100922>
- Arikan, D., & Yıldız, F. (2021, Mayıs). *An Analysis of NO<sub>2</sub> Emission During COVID-19 Period in Turkey*. 11. Türkiye Ulusal Fotogrametri ve Uzaktan Algılama Birliği (TUFUAB) Teknik Sempozyumu, 6-9, Mersin, Türkiye.
- Arikan, D., & Yıldız, F. (2022, Ekim). *Landsat-8 Uyduyu Kullanılarak 2018-2021 Yılları Arasında İstanbul'daki Kentsel Isı Adasının İncelenmesi*. 362-372, İzmir, Türkiye.
- Balmes, J. R. (2019). Household air pollution from domestic combustion of solid fuels and health. *Journal of Allergy and Clinical Immunology*, 143(6), 1979-1987. doi:<https://doi.org/10.1016/j.jaci.2019.04.016>
- Cheung, C. W., He, G., & Pan, Y. (2020). Mitigating the air pollution effect? The remarkable decline in the pollution-mortality relationship in Hong Kong. *Journal of Environmental Economics and Management*, 101, 102316. doi:<https://doi.org/10.1016/j.jeem.2020.102316>
- Dentener, F., Emberson, L., Galmarini, S., Cappelli, G., Irimescu, A., Mihailescu, D., van den Berg, M. (2020). Lower air pollution during COVID-19 lock-down: improving models and methods estimating ozone impacts on crops. *Philosophical Transactions of the Royal Society A*, 378(2183), 20200188. doi:<https://doi.org/10.1098/rsta.2020.0188>
- Farahat, A. (2022). The Impact of the 2020 Oil Production Fluctuations on Methane Emissions over the Gulf Cooperation Council (GCC) Countries: A Satellite Approach. *Atmosphere*, 13(1), 11. doi:<https://doi.org/10.3390/atmos13010011>
- Ghasempour, F., Sekertekin, A., & Kutoglu, S. H. (2021). Google Earth Engine based spatio-temporal analysis of air pollutants before and during the first wave COVID-19 outbreak over Turkey via remote sensing. *Journal of Cleaner Production*, 319, 128599. doi:<https://doi.org/10.1016/j.jclepro.2021.128599>
- Ghasempour, F., Sekertekin, A., & Kutoglu, H. (2021). Effect of first wave COVID-19 outbreak lockdown measures on satellite-based tropospheric NO<sub>2</sub> over Mersin Province, Turkey. *Intercontinental Geoinformation Days*, 2, 16-19.
- Ghahremanloo, M., Lops, Y., Choi, Y., & Mousavinezhad, S. (2021). Impact of the COVID-19 outbreak on air pollution levels in East Asia. *Science of the Total Environment*, 754, 142226. doi:<https://doi.org/10.1016/j.scitotenv.2020.142226>
- Gorelick, N., Hancher, M., Dixon, M., Ilyushchenko, S., Thau, D., & Moore, R. (2017). Google Earth Engine: Planetary-scale geospatial analysis for everyone. *Remote Sensing of Environment*, 202, 18-27. doi:<https://doi.org/10.1016/j.rse.2017.06.031>
- Griffin, D., Zhao, X., McLinden, C. A., Boersma, F., Bourassa, A., Dammers, E., . . . Fioletov, V. (2019). High-resolution mapping of nitrogen dioxide with TROPOMI: First results and validation over the Canadian oil sands. *Geophysical Research Letters*, 46(2), 1049-1060. doi:<https://doi.org/10.1029/2018GL081095>
- Ghasempour, F., Sekertekin, A., & Kutoglu, S. H. (2021). Google Earth Engine based spatio-temporal analysis of air pollutants before and during the first wave COVID-19 outbreak over Turkey via remote sensing. *Journal of Cleaner Production*, 319, 128599. doi:<https://doi.org/10.1016/j.jclepro.2021.128599>
- Hashim, B. M., Al-Naseri, S. K., Al-Maliki, A., & Al-Ansari, N. (2021). Impact of COVID-19 lockdown on NO<sub>2</sub>, O<sub>3</sub>, PM<sub>2.5</sub> and PM<sub>10</sub> concentrations and assessing air quality changes in Baghdad, Iraq. *Science of the Total Environment*, 754, 141978. doi:<https://doi.org/10.1016/j.scitotenv.2020.141978>



- Hu, H., Landgraf, J., Detmers, R., Borsdorff, T., Aan de Brugh, J., Aben, I., . . . Hasekamp, O. (2018). Toward global mapping of methane with TROPOMI: First results and intersatellite comparison to GOSAT. *Geophysical Research Letters*, 45(8), 3682-3689. doi:<https://doi.org/10.1002/2018GL077259>
- lalongo, I., Virta, H., Eskes, H., Hovila, J., & Douros, J. (2020). Comparison of TROPOMI/Sentinel-5 Precursor NO<sub>2</sub> observations with ground-based measurements in Helsinki. *Atmospheric Measurement Techniques*, 13(1), 205-218. doi:<https://doi.org/10.5194/amt-13-205-2020>
- Ibbetson, A., Symonds, P., & Hutchinson, E. (2020). Data to support small area health impact modelling of air pollution in the United Kingdom. *Data in brief*, 29, 105148. doi:<https://doi.org/10.1016/j.dib.2020.105148>
- Kaplan, G., Avdan, Z. Y., & Avdan, U. (2019). Spaceborne nitrogen dioxide observations from the sentinel-5P TROPOMI over Turkey. *Multidisciplinary digital publishing institute proceedings*, 18(1), 4. doi:<https://doi.org/10.3390/ECRS-3-06181>
- Kunt, F., & Dursun, Ş. (2016). Air pollution modelling of Konya City center by using artificial intelligence methods. *Wulfenia Journal*, 23(11), 76-87.
- Kurata, M., Takahashi, K., & Hibiki, A. (2020). Gender differences in associations of household and ambient air pollution with child health: evidence from household and satellite-based data in Bangladesh. *World Development*, 128, 104779. doi:<https://doi.org/10.1016/j.worlddev.2019.104779>
- Li, C., Chen, W., Wang, Y., Wang, Y., Ma, C., Li, Y., Zhai, W. (2022). Mapping winter wheat with optical and SAR images based on Google earth engine in Henan Province, China. *Remote Sensing*, 14(2), 284. doi:<https://doi.org/10.3390/rs14020284>
- Lorente, A., Borsdorff, T., Butz, A., Hasekamp, O., Schneider, A., Wu, L., . . . Pollard, D. F. (2021). Methane retrieved from TROPOMI: improvement of the data product and validation of the first 2 years of measurements. *Atmospheric Measurement Techniques*, 14(1), 665-684. doi:<https://doi.org/10.5194/amt-14-665-2021>
- Lu, M., Schmitz, O., Vaartjes, I., & Karssenber, D. (2019). Activity-based air pollution exposure assessment: differences between homemakers and cycling commuters. *Health & place*, 60, 102233. doi:<https://doi.org/10.1016/j.healthplace.2019.102233>
- Makineci, H. B. (2022). İstanbul İli Merkez İlçelerindeki NO<sub>2</sub> ve CO Emisyonlarının Uzaktan Algılama ve Yersel İstasyon Verileri Kullanılarak İncelenmesi. *Türkiye Uzaktan Algılama Dergisi*, 4(2), 62-74. <https://doi.org/10.51489/tuzal.1160333>
- Rohi, G., & Ofualagba, G. (2020). Autonomous monitoring, analysis, and countering of air pollution using environmental drones. *Heliyon*, 6(1), e03252. doi:<https://doi.org/10.1016/j.heliyon.2020.e03252>
- Safarianzengir, V., Sobhani, B., Yazdani, M. H., & Kianian, M. (2020). Monitoring, analysis and spatial and temporal zoning of air pollution (carbon monoxide) using Sentinel-5 satellite data for health management in Iran, located in the Middle East. *Air Quality, Atmosphere & Health*, 13, 709-719. doi:<https://doi.org/10.1007/s11869-020-00827-5>
- Sager, L. (2019). Estimating the effect of air pollution on road safety using atmospheric temperature inversions. *Journal of Environmental Economics and Management*, 98, 102250. doi:<https://doi.org/10.1016/j.jeem.2019.102250>
- Singh, S., Singh, H., Sharma, V., Shrivastava, V., Kumar, P., Kanga, S., . . . Singh, S. K. (2021). Impact of forest fires on air quality in Wolgan Valley, New South Wales, Australia—a mapping and monitoring study using Google Earth engine. *Forests*, 13(1), 4. doi:<https://doi.org/10.3390/f13010004>
- Slagter, B., Tsendbazar, N.-E., Vollrath, A., & Reiche, J. (2020). Mapping wetland characteristics using temporally dense Sentinel-1 and Sentinel-2 data: A case study in the St. Lucia wetlands, South Africa. *International Journal of Applied Earth Observation and Geoinformation*, 86, 102009. doi:<https://doi.org/10.1016/j.jag.2019.102009>

- Sobhani, B., & Zengir, V. S. (2019). Investigation hazard effect of monthly ferrin temperature on agricultural products in north bar of Iran. *The Iraqi Journal of Agricultural Science*, 50(1), 320-330.  
doi:<https://doi.org/10.36103/ijas.v50i1.298>
- Sobhani, B., & Zengir, V. S. (2020). Modeling, monitoring and forecasting of drought in south and southwestern Iran, Iran. *Modeling Earth Systems and Environment*, 6, 63-71.  
doi:<https://doi.org/10.1007/s40808-019-00655-2>
- Stocker, T. (2014). *Climate change 2013: the physical science basis: Working Group I contribution to the Fifth assessment report of the Intergovernmental Panel on Climate Change*: Cambridge university press.
- Stratoulas, D., & Nuthammachot, N. (2020). Air quality development during the COVID-19 pandemic over a medium-sized urban area in Thailand. *Science of the Total Environment*, 746, 141320.  
doi:<https://doi.org/10.1016/j.scitotenv.2020.141320>
- Theys, N., De Smedt, I., Yu, H., Danckaert, T., van Gent, J., Hörmann, C., . . . Romahn, F. (2017). Sulfur dioxide retrievals from TROPOMI onboard Sentinel-5 Precursor: algorithm theoretical basis. *Atmospheric Measurement Techniques*, 10(1), 119-153.  
doi:<https://doi.org/10.5194/amt-10-119-2017>
- Veeffkind, J. P., Aben, I., McMullan, K., Förster, H., De Vries, J., Otter, G., . . . Kleipool, Q. (2012). TROPOMI on the ESA Sentinel-5 Precursor: A GMES mission for global observations of the atmospheric composition for climate, air quality and ozone layer applications. *Remote Sensing of Environment*, 120, 70-83.  
doi:<https://doi.org/10.1016/j.rse.2011.09.027>
- Wang, H., Gong, F.-Y., Newman, S., & Zeng, Z.-C. (2022). Consistent weekly cycles of atmospheric NO<sub>2</sub>, CO, and CO<sub>2</sub> in a North American megacity from ground-based, mountaintop, and satellite measurements. *Atmospheric Environment*, 268, 118809.  
doi:<https://doi.org/10.1016/j.atmosenv.2021.118809>